In vivo characterization of cortical and white matter neuroaxonal pathology in early multiple sclerosis

Tobias Granberg,[1,2,3,4] Qiuyun Fan,[1,2] Constantina Andrada Treaba,[1,2] Russell Ouellette,[1,3] Elena Herranz,[1,2] Gabriel Mangeat,[1,5] Céline Louapre,[1,2] Julien Cohen-Adad,[1,5] Eric C. Klawiter,[2,6] Jacob A. Sloane[2,7] and Caterina Mainero[1,2]

Neuroaxonal pathology is a main determinant of disease progression in multiple sclerosis; however, its underlying pathophysiological mechanisms, including its link to inflammatory demyelination and temporal occurrence in the disease course are still unknown. We used ultra-high field (7 T), ultra-high gradient strength diffusion and T_1/T_2-weighted myelin-sensitive magnetic resonance imaging to characterize microstructural changes in myelin and neuroaxonal integrity in the cortex and white matter in early stage multiple sclerosis, their distribution in lesional and normal-appearing tissue, and their correlations with neurological disability. Twenty-six early stage multiple sclerosis subjects (disease duration ⩽ 5 years) and 24 age-matched healthy controls underwent 7 T T_2*-weighted imaging for cortical lesion segmentation and 3 T T_1/T_2-weighted myelin-sensitive imaging and neurite orientation dispersion and density imaging for assessing microstructural myelin, axonal and dendrite integrity in lesional and normal-appearing tissue of the cortex and the white matter. Conventional mean diffusivity and fractional anisotropy metrics were also assessed for comparison. Cortical lesions were identified in 92% of early multiple sclerosis subjects and they were characterized by lower intracellular volume fraction ($P = 0.015$ by paired t-test), lower myelin-sensitive contrast ($P = 0.030$ by related-samples Wilcoxon signed-rank test) and higher mean diffusivity ($P = 0.022$ by related-samples Wilcoxon signed-rank test) relative to the contralateral normal-appearing cortex. Similar findings were observed in white matter lesions relative to normal-appearing white matter (all $P < 0.001$), accompanied by an increased orientation dispersion ($P < 0.001$ by paired t-test) and lower fractional anisotropy ($P < 0.001$ by related-samples Wilcoxon signed-rank test) suggestive of less coherent underlying fibre orientation. Additionally, the normal-appearing white matter in multiple sclerosis subjects had diffusely lower intracellular volume fractions than the white matter in controls ($P = 0.029$ by unpaired t-test). Cortical thickness did not differ significantly between multiple sclerosis subjects and controls. Higher orientation dispersion in the left primary motor-somatosensory cortex was associated with increased Expanded Disability Status Scale scores in surface-based general linear modelling ($P < 0.05$). Microstructural pathology was frequent in early multiple sclerosis, and present mainly focally in cortical lesions, whereas more diffusely in white matter. These results suggest early demyelination with loss of cells and/or cell volumes in cortical and white matter lesions, with additional axonal dispersion in white matter lesions. In the cortex, focal lesion changes might precede diffuse atrophy with cortical thinning. Findings in the normal-appearing white matter reveal early axonal pathology outside inflammatory demyelinating lesions.

1 Athinoula A. Martinos Center for Biomedical Imaging, Department of Radiology, Massachusetts General Hospital, Charlestown, MA, USA
2 Harvard Medical School, Cambridge, MA, USA
3 Department of Clinical Neuroscience, Karolinska Institutet, Stockholm, Sweden
4 Department of Radiology, Karolinska University Hospital, Stockholm, Sweden
5 NeuroPoly Lab, Institute of Biomedical Engineering, Polytechnique Montréal, Montreal, QC, Canada
6 Department of Neurology, Massachusetts General Hospital, Boston, MA, USA
7 Department of Neurology, Beth Israel Deaconess Medical Center, Boston, MA, USA

Correspondence to: Caterina Mainero, MD, PhD
A. A. Martinos Center for Biomedical Imaging
149, 13th street
Charlestown, MA 02129, USA
E-mail: caterina@nmr.mgh.harvard.edu

Introduction

Neuroaxonal degeneration in multiple sclerosis is a main determinant of disease progression and an important predictor of the clinical outcome (Filippi *et al.*, 2012). Although MRI is essential in the diagnostic work-up and monitoring of disease course and treatment effects in multiple sclerosis, conventional imaging has limited sensitivity to the microstructural changes that accompany the development of neuroaxonal pathology both in the cortex and white matter, before the establishment of irreversible tissue loss (MAGNIMS Study Group, 2015; Filippi *et al.*, 2016).

The temporal dynamics and pathophysiological mechanisms underlying neuroaxonal degeneration in multiple sclerosis are still uncertain. Axonal and neuronal injury could be the consequence of demyelination with loss of trophic support from oligodendrocytes, but also occur in the absence of focal demyelination, in the so-called normal-appearing tissue (Friese *et al.*, 2014). Increasing neuropathological and imaging evidence suggests that these events could start from the earliest disease stages of multiple sclerosis (Kuhlmann *et al.*, 2002; Lucchinetti *et al.*, 2011; Simon, 2012; Louapre *et al.*, 2014; Guttmann *et al.*, 2016). Studies using non-conventional MRI techniques, such as magnetization transfer and diffusion imaging, have indeed demonstrated the presence of pathological changes in the normal-appearing white matter (NAWM) in all disease stages (Guo *et al.*, 2002; Agosta *et al.*, 2006; Vrenken *et al.*, 2007). These techniques are, however, not able to disentangle the heterogeneous processes that characterize multiple sclerosis pathology.

The non-invasive study of cortical demyelination in multiple sclerosis remains a challenge. Advances in neuroimaging have demonstrated that the detection of cortical demyelinating lesions *in vivo* can be improved through dedicated MRI sequences. Particularly, T_2^* imaging at ultra-high field strength MRI has been shown to have increased sensitivity for subpial lesions and diffuse demyelination relative to other MRI sequences (Pitt *et al.*, 2010; Jonkman *et al.*, 2016; Kilsdonk *et al.*, 2016). Current knowledge of the frequency, distribution and tissue characteristics of cortical lesion pathology in early disease is, however, limited and ultra-high field strength MRI has not yet been systematically applied *in vivo* in studies of early

multiple sclerosis. Furthermore, although previous pathological and advanced imaging studies have shown that cortical grey matter pathology is a main determinant of the clinical outcome in multiple sclerosis, the temporal occurrence of metabolic, micro- and macro-structural pathology in the cortex has yet to be determined (Chard and Miller, 2009). As the foundations of long-term disability may be laid very early in the clinical course of the disease, the ability to track cortical pathological processes *in vivo*, from the earliest disease stages, could prove beneficial for improving disease monitoring.

The neuropathological correlates of cortical lesions in early stage multiple sclerosis are also largely unknown. Previous histopathological examinations described transected neurites and apoptotic neurons associated with cortical demyelination, but these observations mostly derived from progressive multiple sclerosis *ex vivo* samples (Peterson *et al.*, 2001; Bø *et al.*, 2003; Haider *et al.*, 2016). Only one previous study that used biopsies on atypical multiple sclerosis cases at disease onset reported on the presence of cortical demyelinating lesions, including the subpial type, in the earliest disease stages (Lucchinetti *et al.*, 2011). In that work, in addition to demyelination, several cortical lesions showed evidence of neuritic injury, pyknotic neurons, and reduced oligodendrocyte density, all occurring on a background of meningeal inflammation.

The neurite orientation dispersion and density imaging (NODDI) model is a clinically feasible application of recent diffusion MRI models that incorporate multiple shells with different b-values to differentiate between compartments of different length-scales within a voxel. Specifically, NODDI models the water diffusion in three compartments: the free isotropic Gaussian diffusion in CSF or oedema; the hindered anisotropic Gaussian diffusion in the extracellular space; and the restricted anisotropic non-Gaussian diffusion in the intracellular space. NODDI also models the orientation dispersion, inferring information about the underlying orientational coherence or structural integrity of the tissue (Zhang *et al.*, 2012; Colgan *et al.*, 2016). Hence, in contrast to traditional diffusion tensor model metrics (mean diffusivity, fractional anisotropy), the NODDI model allows for biologically specific inference of the microstructural properties of tissues (Assaf *et al.*, 2004, 2008; Sotiropoulos *et al.*, 2012; Zhang *et al.*, 2012).

In this study, we used ultra-high field strength, $7\,T\ T_2^*$ imaging and ultra-high gradient strength diffusion MRI with NODDI modelling to characterize, in early stage multiple sclerosis, the extent and microstructural properties of pathology in the cortex and white matter, both in lesional and normal-appearing tissue. We combined these methods with MRI-based myelin imaging (Alonso-Ortiz *et al.*, 2015), which uses the ratio of T_1- and T_2-weighted images to reduce the effect of field inhomogeneities and obtain a combined myelin-sensitive image contrast (Glasser and Van Essen, 2011; Glasser *et al.*, 2014, 2016).

We hypothesized that demyelination and microstructural neuroaxonal pathology could be detected early in the disease in both the cortex and the white matter. We assessed whether microstructural abnormalities in myelin and neuroaxonal integrity in early stage multiple sclerosis were closely associated in lesional and normal-appearing tissue. In the cortex, we hypothesized that the advanced imaging tools proposed in this study would be more sensitive than conventional diffusion and atrophy assessments in disclosing early cortical microstructural pathology. Finally, we investigated how these different aspects of multiple sclerosis pathology relate to neurological disability.

Materials and methods

Participants and clinical assessments

This prospective cohort study was approved by the local institutional review board and written informed consent was obtained from all participants. General inclusion criteria were: age between 18 and 60 years, absence of significant medical history (other than multiple sclerosis for patients) and of MRI contraindications. Eligibility criteria in patients included a diagnosis of relapsing-remitting multiple sclerosis (Polman *et al.*, 2011; Lublin *et al.*, 2014) with a disease duration $\leqslant 5$ years in line with Chard and Miller (2009), being on stable disease-modifying treatment or no treatment for at least 3 months, absence of clinical relapse within 3 months

and of corticosteroids use within 10 month from study enrolment. We enrolled 50 participants: 26 subjects with early stage multiple sclerosis and 24 age- and gender-matched healthy controls. The demography of the participants is detailed in Table 1. Four healthy controls [one female, three males; mean age 35.3 years, standard deviation (SD) 8.8 years] were recruited for assessing the scan-rescan reproducibility of the diffusion metrics. Physical disability in multiple sclerosis subjects was assessed using the Expanded Disability Status Scale (EDSS) (Kurtzke, 1983).

Image acquisition and analysis

The image processing pipeline is detailed below and summarized in Fig. 1.

Ultra-high gradient strength MRI

All participants were imaged on the 3 T MGH-USC Connectome Scanner (MAGNETOM Skyra CONNECTOM, Siemens Healthcare), using a gradient system that is capable of generating up to 300 mT/m gradient strength (McNab *et al.*, 2013; Setsompop *et al.*, 2013), with a 64-channel head coil (Keil *et al.*, 2013). Multi-shell diffusion-weighted images were acquired using a 2D echo-planar imaging sequence (1.5 mm isotropic voxel size, b-values 1000 and 5000 s/mm^2 with 64 and 128 diffusion weighting directions). We applied higher b-values and number of diffusion weighting directions than in the original NODDI protocol, as previous studies have demonstrated that a high b-value and high angular resolution are beneficial for estimating the orientation dispersion index accurately (Zhang *et al.*, 2012; Fick *et al.*, 2016). The choice of b-values was based on the total acquisition time and the capability of the specific scanner to accommodate stronger diffusion weightings and high angular resolution with short echo times, thus reducing signal loss. Anatomical images were acquired using 3D sequences with 1.0 mm isotropic voxel size: T_1-weighted multi-echo magnetization-prepared rapid gradient-echo images in all participants (van der Kouwe *et al.*, 2008), T_2-weighted images (available in 24 multiple sclerosis subjects and 15 control subjects) and fluid-attenuation inversion recovery (FLAIR) in all multiple sclerosis subjects.

Table 1 Demographic and clinical characteristics of early stage multiple sclerosis subjects and healthy controls

	Multiple sclerosis subjects	Healthy controls
Gender, n (females/males)	26 (21/5)	24 (17/7)[†]
Age, years, mean ± SD	39.0 ± 8.2	37.7 ± 10.6[‡]
Disease duration, years, mean ± SD	2.5 ± 1.4	-
EDSS scores, median (range)	1.5 (0–4)	-
Disease-modifying treatments (n)	Dimethyl fumarate (n = 11)	
	Glatiramer acetate (n = 6)	
	Interferon beta-1a (n = 4)	
	Natalizumab (n = 1)	
	None (n = 4)	

[†]$P = 0.51$ versus multiple sclerosis subjects by Fischer's exact test.
[‡]$P = 0.64$ versus multiple sclerosis subjects by unpaired *t*-test.
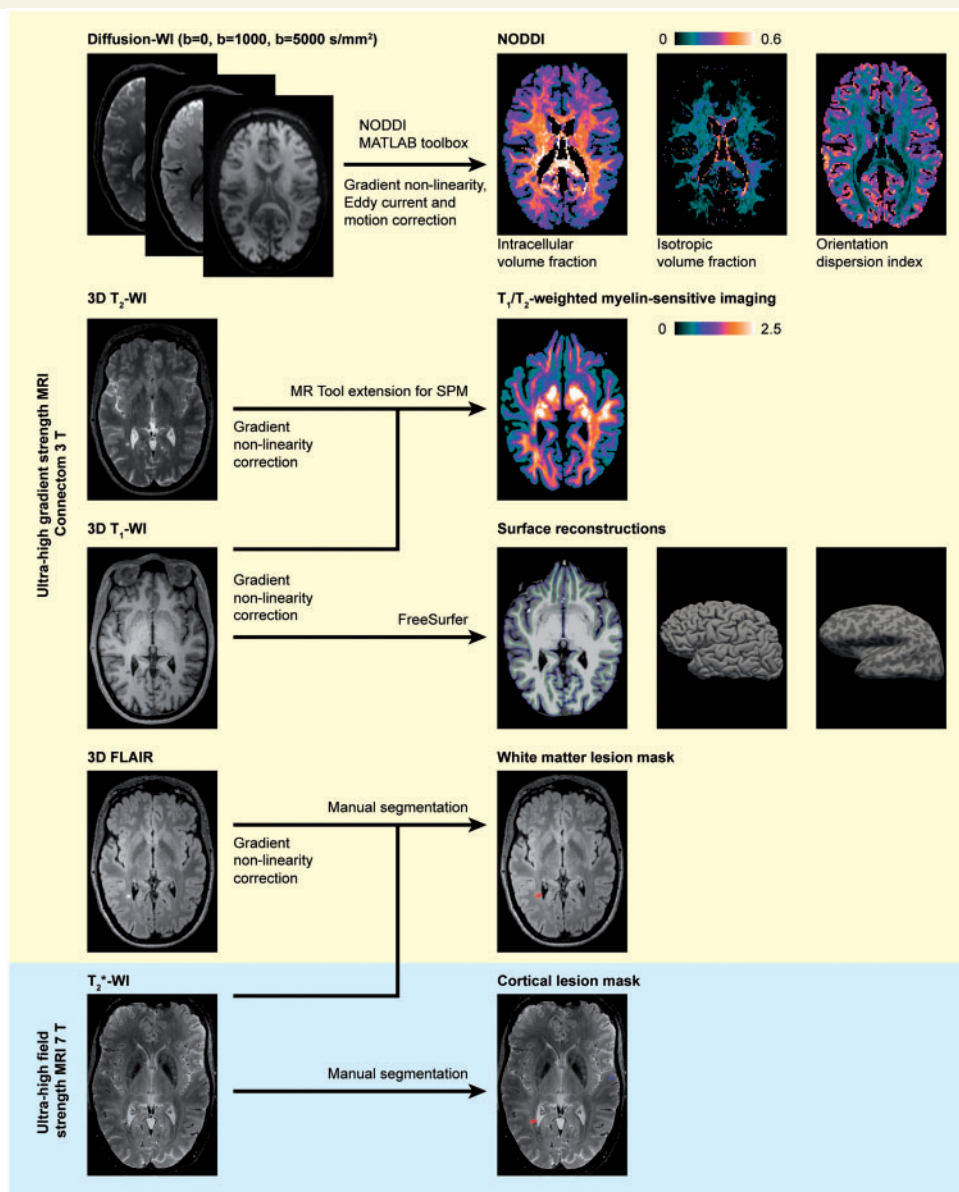SD = standard deviation.

Figure 1 Overview of the image acquisition and processing pipeline. Ultra-high gradient strength MRI processed for NODDI, myelin-sensitive imaging, FreeSurfer reconstruction and lesion masks in a 46-year-old female multiple sclerosis subject with 1.7-year disease duration and an EDSS score of 2. Images presented in the native space for each modality. FLAIR = fluid-attenuated inversion recovery; SPM = statistical parametric mapping; WI = weighted imaging.

Ultra-high field strength MRI

A Siemens 7 T scanner (MAGNETOM, Siemens Healthcare) with a 32-channel head coil was used for imaging 16 controls and all multiple sclerosis subjects except one due to the presence of metallic implants not approved for 7 T. In these subjects, a 2D single-echo fast low-angle shot spoiled T_2^* gradient-echo sequence (two slabs covering the supratentorial brain) was acquired at ultra-high resolution (0.33 × 0.33 × 1.0 mm). Further imaging parameters are listed in Supplementary Table 1.

Cortical surface reconstruction

The 3 T T_1-weighted images were used for cortical surface reconstructions, cortical thickness measurements and for creating masks of the cortex, white matter and CSF in FreeSurfer (v. 5.3.0, http://freesurfer.net) (Fischl, 2012). Topological surface reconstruction defects caused by white matter and leukocortical lesions were corrected with semi-automatic lesion in-painting in FreeSurfer.

Lesion quantification in cortex and white matter

Lesions were manually segmented using Slicer (v. 4.2.0, https://www.slicer.org) (Fedorov et al., 2012), through the consensus of two experienced raters (C.A.T. and C.M.). Cortical lesions were segmented on 7 T images and classified as intracortical or leukocortical as previously detailed (Louapre et al., 2015). White matter lesions were identified primarily on 3 T FLAIR images with the complementing guidance of 7 T T_2^* images.

Examples of lesion segmentations are shown in Fig. 1. Lesion volumes in both white matter and cortex were quantified using fslstats (FMRIB Software Library, FSL, v. 5.0, Oxford, UK, http://fsl.fmrib.ox.ac.uk/fsl). Prior to assessing cortical lesion volumes, cortical lesion masks from the two 7 T T_2^* slabs were registered onto the 3 T anatomical Freesurfer reconstructions using a boundary-based registration method as previously detailed (Greve and Fischl, 2009; Mainero *et al.*, 2015).

Diffusion modelling

Diffusion-weighted images were corrected for gradient non-linearities, eddy-current distortions and for subject motion using interspersed non-diffusion weighted images, as previously detailed (Fan *et al.*, 2016). The diffusion preprocessing pipeline applied here has been optimized and tested to assure a satisfying eddy current artefact correction even at high b-values (Fan *et al.*, 2016), and the results are publicly available online (ConnectomeDB, http://www.humanconnectome.org/software/connectomeDB.html and LONI IDA https://ida.loni.usc.edu). After preprocessing, the two-shell high-angular resolution diffusion-weighted volumes were then analysed using the NODDI toolbox (v. 0.9, University College London, London, UK, http://mig.cs.ucl.ac.uk/mig/mig/index.php/?n=Tutorial.NODDImatlab/) (Zhang *et al.*, 2012). In short, a non-linear three-compartment tissue model was fitted to the diffusion-weighted data where signal contribution of the free isotropic Gaussian diffusion in CSF or oedema (isotropic volume fraction) was separated from the hindered anisotropic Gaussian diffusion in the extracellular space and the restricted anisotropic non-Gaussian diffusion in the intracellular space (intracellular volume fraction). The orientational coherence or structural integrity of the tissues was modelled with a Watson distribution, resulting in the orientation dispersion index. To facilitate comparisons with previous studies with traditional diffusion analysis, the tensor model with weighted least squares using the FDT tool in FSL (https://fsl.fmrib.ox.ac.uk/fsl/fslwiki/FDT/UserGuide#DTIFIT) was fitted to the b = 1000 s/mm² diffusion-weighted data to obtain conventional fractional anisotropy and mean diffusivity measures.

Myelin-sensitive imaging

A method for non-invasive myelin-sensitive imaging was applied where the T_1- and T_2-weighted sequences were processed to obtain a myelin-sensitive contrast (Glasser and Van Essen, 2011; Glasser *et al.*, 2014), using the MR Tool - Multimodal Mapping extension (v. 1.2, Swiss Federal Institute of Technology, Zurich, Switzerland, http://www.fil.ion.ucl.ac.uk/spm/ext) for Statistical Parametric Mapping 12 (University College London, London, UK, http://www.fil.ion.ucl.ac.uk/spm). Briefly, the processing includes bias correction and rigid registration of the T_2-weighted images to the T_1-weighted images with linear calibration of image intensity modes using non-brain tissue masks to produce a normalized MRI-based myelin-sensitive imaging contrast that uses the ratio of T_1- and T_2-weighted images (Ganzetti *et al.*, 2014, 2015).

Analysis of diffusion and myelin-sensitive imaging in white matter and cortex

Individual maps of diffusion-based metrics were registered via their corresponding non-diffusion weighted echo-planar images to the cortical FreeSurfer reconstructions using boundary-based registration with 12 degrees of freedom (Greve and Fischl, 2009). The same tool was used to rigidly register the myelin-sensitive contrasts to the FreeSurfer reconstructions. For the purpose of studying cortical pathology specifically, only the intracortical portion of leukocortical lesions was considered by applying the anatomical cortical mask from FreeSurfer so that only the part of the lesions confined between the grey–white matter border and the pial surface was included (illustrated in Supplementary Fig. 1). To minimize partial volume effects due to the thin and convoluted shape of the cerebral cortex, a surface-based approach was also used where NODDI metrics and myelin-sensitive image intensities were sampled across the whole cortex at mid-cortical depth (50% of the distance between the FreeSurfer pial and white matter surface reconstructions).

Since T_1/T_2-weighted myelin-sensitive imaging and diffusion metrics are known to differ topographically across the brain (Ganzetti *et al.*, 2014; Glasser *et al.*, 2014, 2016), imaging metrics in cortical and/or white matter lesions were compared with the homologous non-lesioned tissue in the contralateral region. The original T_1-weighted images and its right–left inverted 'mirror' image were both non-linearly registered to the MNI152 T_1-weighted 1 mm brain template (Montreal Neurological Institute, Montreal, Canada, http://www.bic.mni.mcgill.ca/ServicesAtlases/ICBM152NLin2009) using FNIRT in FSL to find the contralateral homologous correspondence, and the non-linear warp fields were concatenated to calculate the masks of the contralateral non-lesioned homologous areas.

Scan-rescan reproducibility of diffusion metrics

Since NODDI is a relatively recent diffusion model and it has yet sparsely been used for clinical applications, the scan-rescan reproducibility of diffusion metrics, both in the cortex and in white matter, was assessed in four healthy volunteers by acquiring the diffusion-weighted scans twice, in the same day, with a short time interval between the two imaging sessions, and with repositioning of subjects. The absolute difference in diffusion metrics was calculated as: |(Scan 1 − Scan 2)|. The within-subject coefficient of variations was estimated, both in the cortex and in the white matter, as the ratio between the standard deviation and the mean of each couple (Scan 1, Scan 2) of measurements. In the cortex, the reproducibility of diffusion metrics was assessed either in the volume space, which was defined as the cortical volume between the white–grey matter boundary and the pial surface, or in the surface-based space, by sampling metrics at mid-cortical depth as previously detailed (Govindarajan *et al.*, 2015).

Statistical analysis

Statistical analysis was performed in IBM SPSS Statistics 23 for Mac (IBM, Armonk, USA). Shapiro-Wilk's test was used to assess normality. Group differences in nominal data were assessed with Fisher's exact test, unpaired parametric data using unpaired *t*-test and unpaired non-parametric data using independent-samples Mann-Whitney U-test. Paired analyses within subjects of lesioned and non-lesioned homologous regions

averaged per subject were compared with paired *t*-test for parametric data and related samples Wilcoxon signed rank test for non-parametric data. Since the lesion count in patients was heterogeneous, intralesional NODDI and myelin-sensitive metrics were averaged per subject. Bivariate correlations were analysed with Pearson correlation for parametric data and Spearman's rank correlation coefficient for non-parametric data. A two-tailed $P < 0.05$ was considered statistically significant.

Surface-based group analysis of cortical thickness, NODDI and myelin-sensitive metrics

For surface-based group analyses of cortical thickness, NODDI metrics and myelin-sensitive contrast across the whole cortex, individual surfaces of each metric were registered to a common template surface (fsaverage) and a smoothing kernel of 10 mm full-width at half-maximum was applied. A general linear model was used to assess vertex-wise across the entire cortex: (i) differences in cortical thickness, NODDI metrics and myelin-sensitive contrast between multiple sclerosis subjects and controls; and (ii) associations of cortical thickness, NODDI metrics and myelin-sensitive contrast with EDSS in multiple sclerosis subjects. To mediate any possible partial volume effects caused by atrophy, the surface-based general linear models with NODDI metrics and myelin-sensitive contrast were corrected for the cortical thickness on a per-vertex basis. In all analyses, a correction for multiple comparisons was applied through Monte Carlo null-z simulation with 10 000 iterations and a significance level of $P < 0.05$.

Results

Cortical thickness and lesions in the cortex and white matter

Lesion counts and volumes in the multiple sclerosis cohort are summarized in Table 2. Cortical lesions were identified in 23 of 25 multiple sclerosis subjects (92%), and in none of the controls. In terms of cortical lesion subtypes, intra-cortical lesions were found in 17 multiple sclerosis subjects (68%) and leukocortical lesions were also found in 17 multiple sclerosis subjects (68%). The distribution of cortical lesions across the cortex is presented in Fig. 2.

Table 2 Lesion counts and volumes in the cortex and white matter of early stage multiple sclerosis subjects

	Median (range)	Mean ± SD
Cortical lesion count	2 (0–39)	6.0 ± 9.5
Cortical lesion volume	134 (0–2190)	289 ± 493
Intracortical lesion count	2 (0–32)	4.3 ± 8.0
Intracortical lesion volume	81 (0–1650)	194 ± 384
Leukocortical lesion count	1 (0–7)	1.6 ± 1.8
Leukocortical lesion volume	28 (0–738)	95 ± 175
White matter lesion count	19 (4–188)	31 ± 37
White matter lesion volume	670 (100–5212)	1098 ± 1306

All volumes are given in mm^3.

Supplementary Fig. 2 shows an example of an early multiple sclerosis subject with a high cortical lesion load. The white matter lesion volume correlated with the leukocortical lesion volume (Spearman's ρ 0.44, $P = 0.026$), but not with the intracortical lesion volume (Spearman's ρ 0.07, $P = 0.74$). Multiple sclerosis subjects exhibited global cortical thinning relative to controls, but this did not reach statistical significance (2.396 ± 0.08 versus 2.434 ± 0.08 mm, unpaired *t*-test $P = 0.12$), and there was also no significant difference in cortical thickness in the surface-based general linear model group comparison.

Diffusion metrics in cortex and white matter

The diffusion metrics in multiple sclerosis subjects and healthy controls, and *P*-values from statistical group comparisons are shown in Table 3 and Fig. 3. The scan-rescan reproducibility of diffusion metrics in the cortex and white matter are reported in Supplementary Table 2.

Cortical lesions were characterized by significantly lower intracellular volume fraction and higher mean diffusivity than the homologous contralateral non-lesioned cortex. There were, however, no significant differences in diffusion metrics in the normal-appearing cortex of multiple sclerosis subjects compared with the cortex of controls. There was also no significant difference in the surface-based model across the whole cortex with NODDI metrics sampled at mid-cortical depth. There was, interestingly, a notable topographical organization of the NODDI metrics across the cortex in both groups, specifically with clear banding of the metrics around the central sulci, in the sensorimotor cortex (Fig. 4).

In the white matter, the intracellular volume fraction in lesions was significantly reduced by 27% compared with the contralateral NAWM. White matter lesions were also characterized by increased mean diffusivity, reflecting increased overall diffusion in the tissues. Furthermore, the orientation dispersion index was increased and the fractional anisotropy decreased, indicating less coherent underlying fibre orientation and suggestive of axonal fanning. NODDI also detected diffuse white matter changes, with a significantly lower intracellular volume fraction in the normal-appearing tissue of multiple sclerosis subjects relative to the white matter of control subjects.

Myelin-sensitive imaging in cortex and white matter

The myelin-sensitive imaging results and *P*-values from statistical group comparisons are presented in Table 3 and visualized in Fig. 3. In the cortex, lesions had significantly reduced myelin-sensitive image contrast compared with the contralateral non-lesioned cortex. There were no significant differences between the myelin-sensitive contrast in the normal-appearing cortex in multiple sclerosis subjects and the cortex in the controls. No significant difference was
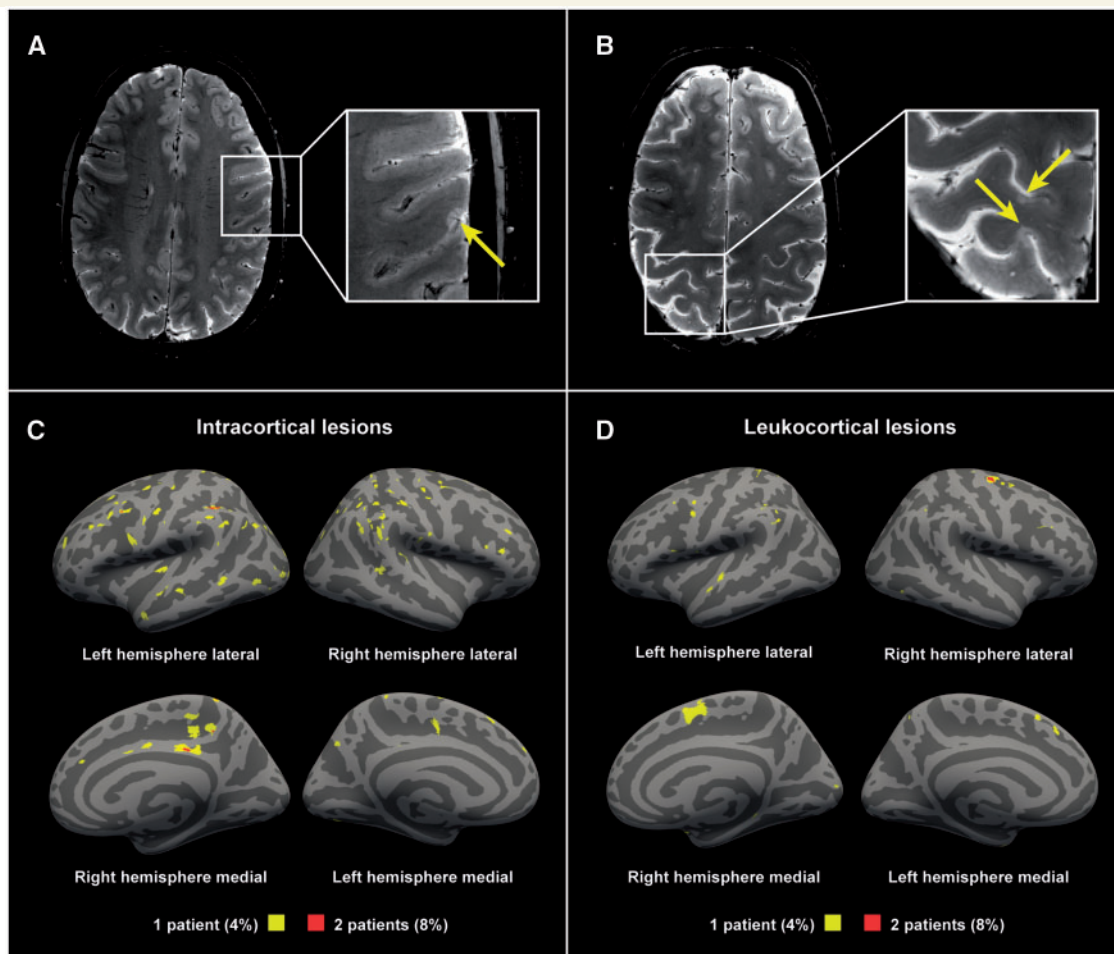
Figure 2 Examples of cortical lesions detected with 7 T T$_2$*-weighted imaging. (**A**) A 36-year-old female multiple sclerosis subject with a disease duration of 1.8 years, EDSS score of 0; (**B**) A 45-year-old female multiple sclerosis subject with a disease duration of 2.9 years, an EDSS score of 3. Lesion probability maps of (**C**) intracortical lesions and (**D**) the cortical portion of leukocortical lesions in all multiple sclerosis subjects displayed on fsaverage. Yellow indicating lesions in 4% (1 of 25 subjects). Red indicating 8% (2 of 25 subjects) having overlapping lesions (maximum overlap).

found in the surface-based comparisons across the whole cortex between multiple sclerosis subjects and controls either. However, as illustrated in Fig. 4, a trend of lower myelin-sensitive contrast in the superior frontoparietal regions was visually noted in multiple sclerosis subjects compared with controls.

In the white matter, lesions had a marked and significant reduction (37%) in the myelin-sensitive contrast, suggestive of reduced myelin content, compared with the contralateral non-lesioned white matter areas. No significant differences were, however, found between the myelin-sensitive contrast in the NAWM of multiple sclerosis subjects and the white matter of controls.

Correlations with neurological disability

In the surface-based general linear modelling, there was a positive association between the orientation dispersion

index in the left primary motor and somatosensory cortices and EDSS scores (Fig. 5), which remained significant after correction for multiple comparisons and the cortical thickness on a per-vertex basis. The remaining NODDI metrics, myelin imaging and cortical thickness did not show any significant associations with the EDSS scores.

Discussion

In this study, we combined ultra-high field 7 T and ultra-high gradient strength diffusion MRI along with T$_1$/T$_2$-weighted myelin-sensitive imaging to characterize myelin and neuroaxonal integrity in the brain of early stage multiple sclerosis subjects.

We found that the cortex is commonly affected by focal lesions in early multiple sclerosis (92% of multiple sclerosis subjects) and that myelin-sensitive image contrasts and advanced diffusion modelling can be helpful in characterizing *in vivo* microstructural tissue changes that accompany

Table 3 Results from diffusion modelling and myelin-sensitive imaging in the cortex and in the white matter of early stage multiple sclerosis subjects and healthy controls

	Multiple sclerosis lesions	Contralateral normal-appearing tissue		Whole normal-appearing tissue, multiple sclerosis subjects	Whole normal-appearing tissue, controls	
Cortex						
Myelin-sensitive intensity	1.06 ± 0.176	1.17 ± 0.182	$P = 0.030^{\dagger}$	1.09 ± 0.144	1.12 ± 0.143	$P = 0.70^{\S}$
Intracellular volume fraction	0.408 ± 0.047	0.441 ± 0.050	$P = 0.015*$	0.432 ± 0.017	0.431 ± 0.015	$P = 0.84^{\ddagger}$
Isotropic volume fraction	0.041 ± 0.077	0.025 ± 0.049	$P = 0.78^{\dagger}$	0.089 ± 0.031	0.091 ± 0.025	$P = 0.56^{\S}$
Orientation dispersion index	0.508 ± 0.078	0.525 ± 0.068	$P = 0.30*$	0.544 ± 0.009	0.544 ± 0.007	$P = 0.98^{\ddagger}$
Fractional anisotropy	0.186 ± 0.054	0.184 ± 0.050	$P = 0.29^{\dagger}$	0.181 ± 0.012	0.182 ± 0.006	$P = 0.85^{\S}$
Mean diffusivity	0.788 ± 0.087	0.730 ± 0.097	$P = 0.022^{\dagger}$	0.795 ± 0.070	0.809 ± 0.031	$P = 0.59^{\S}$
White matter						
Myelin-sensitive intensity	1.32 ± 0.275	2.11 ± 0.312	$P = 1.8 \times 10^{-5\dagger}$	2.25 ± 0.380	2.55 ± 0.653	$P = 0.25^{\S}$
Intracellular volume fraction	0.478 ± 0.057	0.655 ± 0.061	$P = 4.8 \times 10^{-13}*$	0.622 ± 0.023	0.638 ± 0.027	$P = 0.029^{\ddagger}$
Isotropic volume fraction	0.166 ± 0.069	0.151 ± 0.055	$P = 0.32^{\dagger}$	0.108 ± 0.033	0.108 ± 0.032	$P = 0.95^{\S}$
Orientation dispersion index	0.276 ± 0.033	0.259 ± 0.038	$P = 3.0 \times 10^{-5}*$	0.300 ± 0.014	0.297 ± 0.015	$P = 0.43^{\ddagger}$
Fractional anisotropy	0.367 ± 0.066	0.478 ± 0.081	$P = 8.0 \times 10^{-6\dagger}$	0.439 ± 0.036	0.453 ± 0.290	$P = 0.18^{\S}$
Mean diffusivity	0.934 ± 0.139	0.770 ± 0.119	$P = 9.0 \times 10^{-6\dagger}$	0.714 ± 0.079	0.718 ± 0.041	$P = 0.66^{\S}$

Mean ± SD reported. Mean diffusivity reported as $\mu m^2/s$. *By paired t-test. †By related-samples Wilcoxon signed rank test. ‡By unpaired t-test. §By independent-samples Mann-Whitney U-test.

early cortical lesion pathology. Current knowledge on the distribution and frequency of focal cortical lesions in early disease stages relies mainly on conventional field strength MRI and sparse *ex vivo* case studies (Calabrese *et al.*, 2010*a*; Lucchinetti *et al.*, 2011). At clinical field strengths, dedicated MRI sequences, including double-inversion recovery and phase-sensitive inversion recovery, have shown that cortical lesions can be detected in both clinically and radiologically isolated syndromes at a prevalence of around one-third, with higher frequencies of around two-thirds in more advanced relapse-remitting multiple sclerosis stages (Calabrese *et al.*, 2010*b*; Giorgio *et al.*, 2011). Histopathologically, cortical demyelination has been found *en passant* in the biopsy needle trajectory in ~40% of subjects with atypical multiple sclerosis onset when performing diagnostic biopsies of white matter lesions (Lucchinetti *et al.*, 2011). Previous work has shown that the higher signal-to-noise ratio and resolution achieved at 7 T allows improved cortical lesion delineation in multiple sclerosis, and that the increased T_2*-effects at ultra-high field strength can be used to increase the sensitivity to focal and diffuse cortical pathology in the disease (Mainero *et al.*, 2009; Cohen-Adad *et al.*, 2011; Harrison *et al.*, 2015; Louapre *et al.*, 2015; Kilsdonk *et al.*, 2016). In the current study, using T_2*-weighted imaging at 7 T MRI, we found that cortical lesions were present in almost all multiple sclerosis subjects, suggesting that ultra-high field MRI can greatly improve the ability to disclose early focal cortical pathology in multiple sclerosis.

The frequency of early focal cortical pathology reported in the current study is higher than that reported in the only neuropathological study of early multiple sclerosis thus far (Lucchinetti *et al.*, 2011). Such a discrepancy may be due to the fact that non-invasive imaging methods allow for examination of the entire brain compared with invasive pathological assessments, which are inherently constrained to local brain tissue sampling. The patient cohorts also differ as we included participants with multiple sclerosis representative of a typical clinical population, while the brain tissue sampling was performed in atypical multiple sclerosis cases that underwent biopsy for diagnostic purposes. Despite the high frequency of focal cortical lesion pathology, cortical thickness measured in our cohort, was not statistically different relative to controls. Cortical thickness measurements obtained in our multiple sclerosis cohort are, however, in line with those reported previously in clinically isolated syndrome and early relapsing-remitting multiple sclerosis (Calabrese *et al.*, 2007, 2015; Steenwijk *et al.*, 2014; Nygaard *et al.*, 2015; Pareto *et al.*, 2015). Overall, our findings emphasize that, especially in small multiple sclerosis cohorts, the use of ultra-high resolution protocols at 7 T can significantly improve the ability to disclose early, focal cortical pathological changes, which can then be targeted with more advanced assessments of microstructural integrity. Our findings, thus, highlight the clinical value of cortical lesion imaging, in line with recent recommendations (Filippi *et al.*, 2016). Interestingly, we found that the leukocortical, but not the intracortical, lesion volume correlated with the white matter lesion volume, suggesting that leukocortical lesions may share common pathological substrates with white matter lesions, while intracortical pathology may be a more independent entity. Similarly, the abovementioned biopsy study has also shown a spatial decoupling of cortical and white matter demyelination in early multiple sclerosis (Lucchinetti *et al.*, 2011).
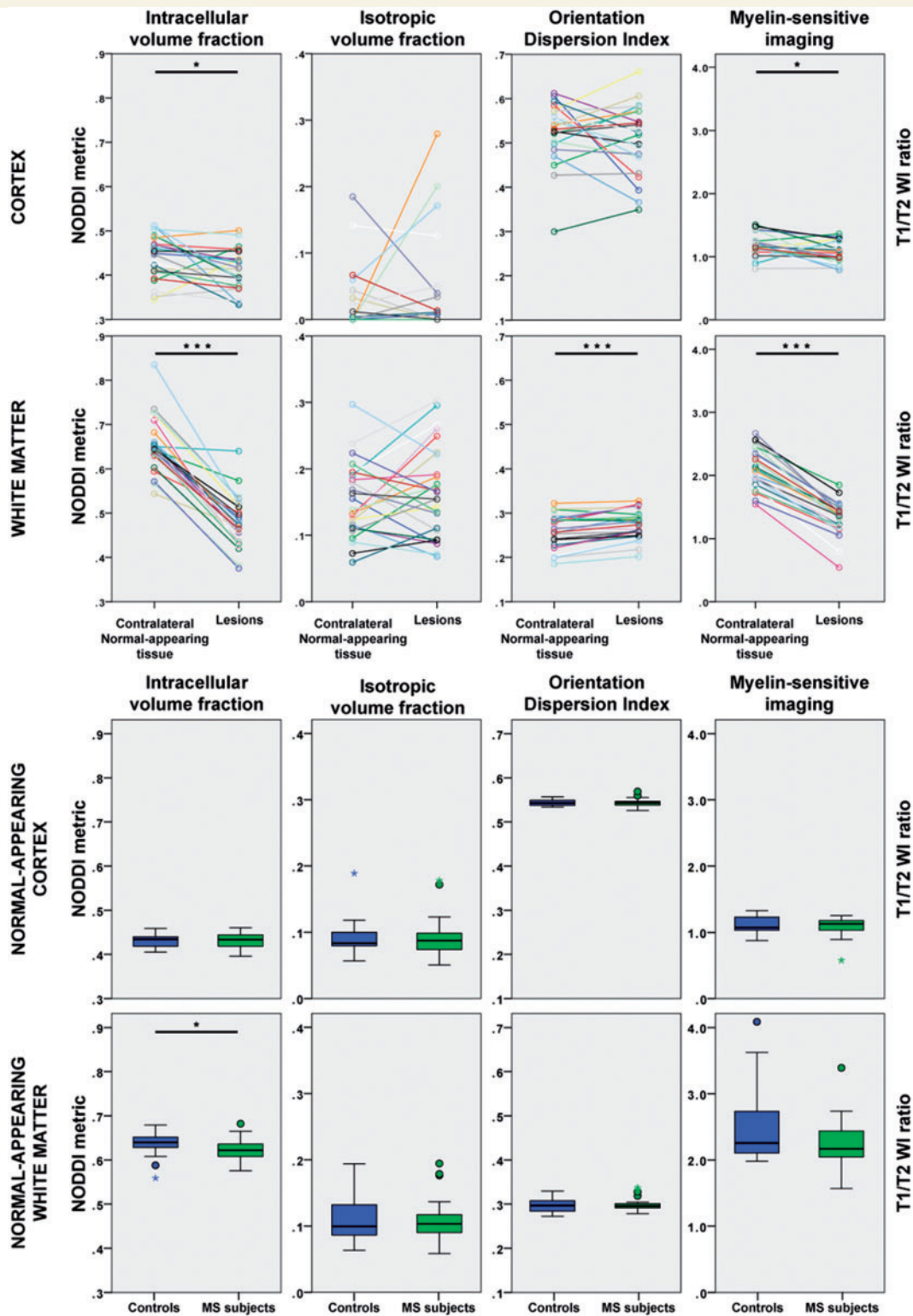
Figure 3 NODDI and myelin-sensitive imaging metrics in the cortex and in the white matter of early stage multiple sclerosis subjects and healthy controls. *$P < 0.05$; ***$P < 0.001$. MS = multiple sclerosis; WI = weighted imaging.

We used myelin-sensitive imaging and advanced diffusion modelling to characterize *in vivo*, in the cortex and white matter, microstructural pathological changes related to disruption of myelin and neuroaxonal integrity. In our early multiple sclerosis cohort, we found lower myelin-sensitive contrast in focal lesions in the cortex, and more profoundly so in white matter. Using NODDI modelling, we also measured significant reductions in the intracellular diffusion
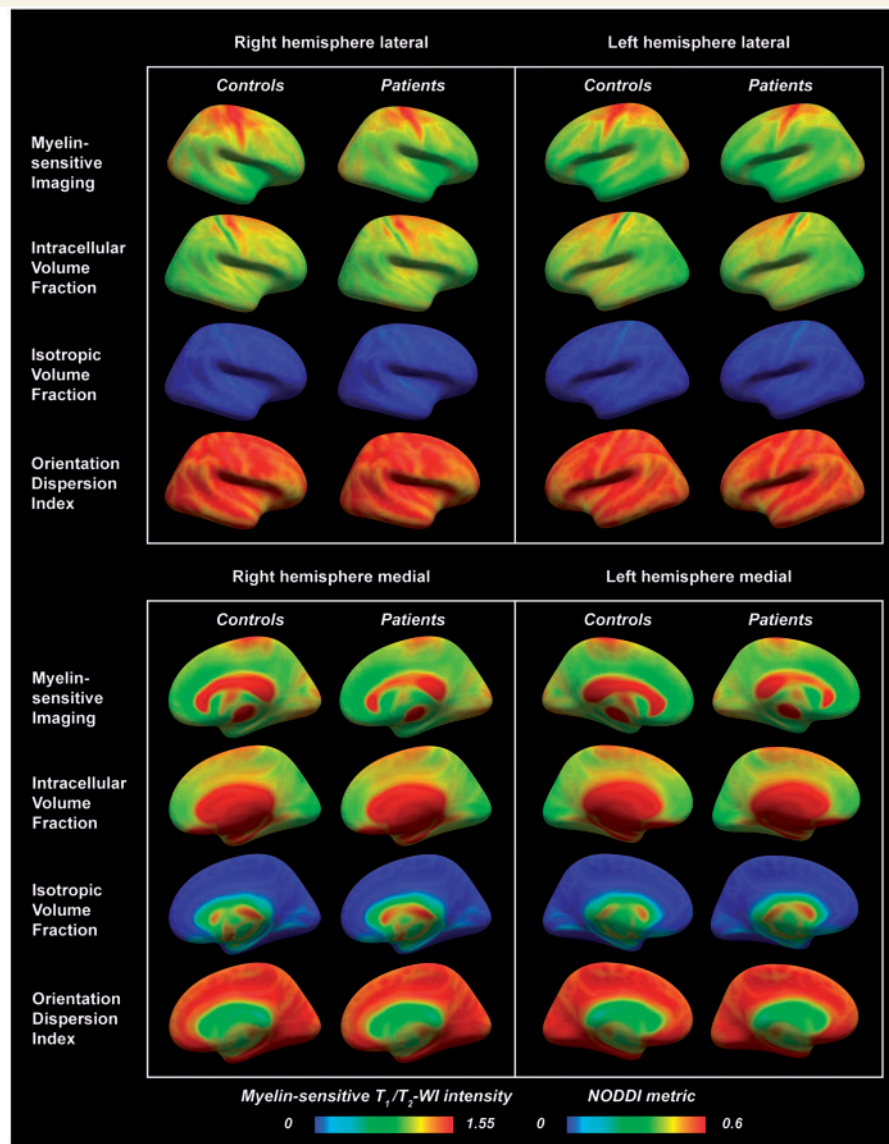
Figure 4 Lateral and medial views in right and left hemispheres of myelin-sensitive imaging and NODDI metrics sampled at mid-cortical depth in multiple sclerosis subjects and healthy controls and displayed on fsaverage. A trend of lower myelin-sensitive contrast in the superior frontoparietal regions was visually noted in multiple sclerosis subjects compared with controls (blue arrows). A notable topographical organization of the NODDI metrics was seen across the cortex, specifically with clear banding of the metrics in the sensorimotor cortices (purple arrows). WI = weighted imaging.

compartment in both cortical and white matter lesions compared with homologous non-lesioned areas. These results could reflect underlying loss and/or smaller size of neurites. The use of additional diffusion models, such as AxCaliber, could be helpful in disentangling density and diameter quantities, though at the cost of lower robustness (Assaf *et al.*, 2008). However, findings from these models in diseased human tissue need to be confirmed pathologically.

Interestingly, despite the lower intracellular volume fraction, in our multiple sclerosis cohort, cortical lesions did not show any significant difference in the fractional anisotropy relative to the contralateral normal-appearing cortex.

This suggests that the lower intracellular volume fraction may be more sensitive than the fractional anisotropy in disclosing early cortical microstructural changes, as previously demonstrated for the white matter (Chung *et al.*, 2016). In our cohort, cortical lesions were also characterized by increased mean diffusivity, which may be a secondary effect to the loss of microstructural integrity and neurites, facilitating free diffusivity, or reflect an increased inflammatory free water component. Previous diffusion studies in multiple sclerosis have reported increased fractional anisotropy, and a few also reported increased mean diffusivity, in cortical lesions (Poonawalla *et al.*, 2008; Calabrese *et al.*, 2011; Filippi *et al.*, 2013; Jonkman
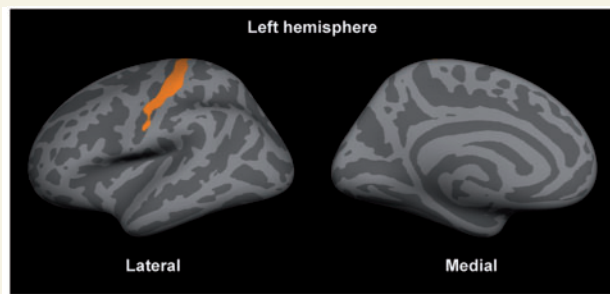
Figure 5 The orientation dispersion index in the primary somatosensory area in the left hemisphere was positively correlated with the expanded disability status scale scores. The significant cluster (after correction for multiple comparisons and the cortical thickness) is displayed on fsaverage.

et al., 2016; Yaldizli *et al.*, 2016). There are some methodological differences between those studies and ours: (i) we focused on early-stage multiple sclerosis, where cortical pathology may be less pronounced than in more advanced disease stages; (ii) we used high resolution diffusion scans with 2–5 times higher spatial resolution compared to previous studies (Calabrese *et al.*, 2011; Filippi *et al.*, 2012; Yaldizli *et al.*, 2016); and (iii) we delineated cortical lesions using 7 T T_2* imaging, which has been shown to exhibit relatively high sensitivity for cortical pathology and may therefore have been able to detect lesions with less severe tissue destruction compared to previous techniques (Mainero *et al.*, 2009; Cohen-Adad *et al.*, 2011; Harrison *et al.*, 2015; Louapre *et al.*, 2015; Kilsdonk *et al.*, 2016). In white matter lesions, lower intracellular volume fraction was accompanied by increased mean diffusivity and orientation dispersion, as well as lower fractional anisotropy, suggesting a combination of demyelination, axonal loss and less coherent fibre orientation such as in axonal bending or fanning in the microenvironment, in agreement with previous histopathological studies of white matter lesions in multiple sclerosis (Schmierer *et al.*, 2007).

We did not find significant group differences in myelin contrast of normal-appearing tissue, neither in the cortex nor in white matter. The intracellular volume fraction measured with NODDI, however, was diffusely lower in the NAWM of multiple sclerosis subjects compared with the white matter of controls. This finding, together with the absence of significant abnormalities in the myelin-sensitive imaging contrast, could be interpreted to reflect the presence of early axonal pathology outside inflammatory demyelinating lesions. It is possible, however, that the T_1/T_2-weighted imaging may be less specific to myelin in white matter than in the cortex (Arshad *et al.*, 2017), and that subtle inflammation with associated demyelination could also be expected to affect the diffusion modelling (Stikov *et al.*, 2015; Jelescu *et al.*, 2016). Axonal transection could indeed occur within inflammatory demyelination, where it

could trigger distal axonal Wallerian degeneration in normal-appearing tissue (Trapp *et al.*, 1998). According to some experimental and pathological studies, however, the pathogenesis of axonal injury in multiple sclerosis may also be independent of inflammatory demyelination (Criste *et al.*, 2014), and reflect the consequence of disturbances in the trophic interactions between oligodendrocytes, microglia and neurons (Trapp and Nave, 2008; Lassmann, 2013).

Our diffusion and myelin-sensitive imaging findings in the cortex highlight the presence of a pathological process that, in the early stages of multiple sclerosis, is more focal than that occurring in the underlying white matter, and predominantly confined to cortical lesions. We previously reported, in another early stage multiple sclerosis cohort (≤3 years disease duration), focal cortical increases in quantitative T_2* at 7T, indicative of underlying myelin and/or iron loss (Mainero *et al.*, 2015). In the current study, the decreased intracellular volume fraction and myelin-sensitive contrast found in cortical lesions relative to homologous normal-appearing tissue suggest the presence of an early reduction in the neurite density along with cortical demyelination. This is in line with pathology reports that described lower neurite, glial and synaptic density in cortical demyelinating lesions in early stage multiple sclerosis (Lucchinetti *et al.*, 2011). Our NODDI results are particularly informative because, unlike traditional diffusion measurements, NODDI takes into account the orientation dispersion in the diffusion property estimates. Additionally, NODDI specifically models the isotropic diffusion, reducing the risk of CSF contributing to the signal. In comparison with previous studies, we acquired high spatial resolution diffusion-weighted images, which also reduces the risk of partial volume contamination with cerebral fluid and white matter. The use of a surface-based method for sampling NODDI metrics and myelin-sensitive contrast at mid-cortical depth also further reduces partial volume effects by accounting for the convoluted shape of the cortex.

The myelin-sensitive imaging method applied in this study has been shown to reflect the distribution of known myelin content across the cortex (Glasser and Van Essen, 2011). A previous histopathological validation demonstrated its sensitivity to cortical demyelination in a small series of multiple sclerosis cases (Nakamura *et al.*, 2016). The method takes advantage of the fact that the T_1-weighted signal is positively correlated with myelin and the T_2-weighted negatively so, making the ratio of the two weightings more myelin-sensitive. Although this contrast is not an absolute measurement of myelin content, and may also reflect iron content, the distribution of cortical iron co-localizes with the myelin distribution and can therefore be thought to indirectly reflect myelin content (Fukunaga *et al.*, 2010; Glasser *et al.*, 2014). There are other MRI-based measurements of myelin content that may be more specific, but these methods require dedicated, often time-consuming, sequences and the histopathologically validated reference method has limited

spatial resolution. The T_1/T_2-weighted myelin-sensitive imaging applied here has a resolution more feasible for studies of the cortex (Glasser *et al.*, 2016), and is based on sequences recommended for clinical use (Rovira *et al.*, 2015; Traboulsee *et al.*, 2016), thus facilitating clinical applications.

In alignment with previous studies (Glasser and Van Essen, 2011; Ganzetti *et al.*, 2014, 2015; Glasser *et al.*, 2014; Mangeat *et al.*, 2015), we found particularly high myelin-related contrast in the primary motor, somatosensory, visual and auditory areas in both multiple sclerosis subjects and controls. Interestingly, we further observed a clear topographical distribution of all NODDI metrics across the cortex in both groups, especially in the primary somatosensory areas where the precentral gyrus was characterized by higher intracellular volume fraction, reflecting overall large cells/dendrites (Fig. 4). This corresponds well with the known cortical cytoarchitecture, with larger neurons being distributed prevalently in the precentral gyrus compared with the postcentral gyrus where there are more glial cells and fewer large neurons (Henderson *et al.*, 1980). This pattern was accompanied by high orientation dispersion and higher myelin-sensitive contrast in the motor cortex. Taken together, these observations indicate that both T_1/T_2-weighted myelin-sensitive imaging and NODDI can prove valuable tools to assess myelin and cytoarchitectural integrity in the healthy brain or in neurological disorders (Kamagata *et al.*, 2015; Caverzasi *et al.*, 2016; Glasser *et al.*, 2016; Morris *et al.*, 2016; Calabrese *et al.*, 2017).

In this study, we investigated associations between metrics from ultra-high field and gradient strength MRI with neurological disability in early stage multiple sclerosis. While we did not detect any clinical association with microstructural pathology in focal cortical and white matter lesions or with cortical thickness, we found that increased orientation dispersion index in the left motor cortex correlated with worsening of EDSS. These findings suggest that, for the cortex, the use of more advanced imaging metrics could prove more sensitive than conventional imaging metrics in disclosing associations with clinical outcome metrics, especially in early disease when functional compensatory mechanisms may be in place to counteract initial neuroaxonal pathology (Pantano *et al.*, 2002; Rocca *et al.*, 2002).

This study has some limitations. Application of NODDI modelling in the white matter and in the cortex is still in its infancy, and histopathological MRI correlative studies are further needed to provide a more definite interpretation of our findings, especially in cortical lesions. Nevertheless, these techniques demonstrate to be quite sensitive to the pathological events that occur in the cortex and in the white matter in the early stages of multiple sclerosis. Time-optimized NODDI protocols could facilitate the use of this advanced imaging method in the clinical setting (Zhang *et al.*, 2012). Converting the complex mathematical modelling of NODDI into linear solutions for greatly accelerated processing is also likely to help the dissemination of

the technique (Daducci *et al.*, 2015). Newer models that calculate microstructural metrics from signal derivatives, rather than fitting the model directly to the data, could be computationally more efficient, and possibly less biased to the intrinsic diffusivity in brain tissue than NODDI (Kaden *et al.*, 2016; Reisert *et al.*, 2017). However, the applicability of these models in pathological tissues remains to be studied and there are noticeable systematic differences in the results between the models that warrants further comparison.

Due to their good reproducibility, NODDI metrics could also be valuable for studying the neuroaxonal pathology in multiple sclerosis longitudinally. Interestingly, in line with previous studies (Zhang *et al.*, 2012; Chung *et al.*, 2016), we found that, among all NODDI metrics, the smallest diffusion compartment, the isotropic volume fraction, showed the highest variability. Ideally, the spatial resolution of the diffusion weighted images should be reduced even further for cortical analyses. Finally, the first 7 T system approved for clinical use has been recently launched, and this will make ultra-high field MRI more common and available in clinic in the near future. Further work, however, needs to be done in order to improve imaging of cortical lesions, even at 7 T, as previous histopathological-MRI correlative studies reported contrasting prospective and retrospective sensitivities to cortical multiple sclerosis lesions even when using the same magnetic resonance contrast (Pitt *et al.*, 2010; Kilsdonk *et al.*, 2016).

In conclusion, we found that in early stage multiple sclerosis there are frequent microstructural abnormalities in neuroaxonal integrity, which are present focally in the cortex and more diffusively in the white matter. Specifically, the results suggest early demyelination with loss of cells and/or cell volumes in cortical and white matter lesions, with additional axonal dispersion in white matter lesions. In the cortex, focal lesion changes might precede diffuse atrophy with cortical thinning. Findings in the NAWM reveal early axonal pathology outside focal demyelinating lesions. Our study suggests that the combined use of ultra-high field 7 T and gradient strength diffusion MRI with NODDI modelling, along with myelin-sensitive imaging, is a valuable and sensitive method for non-invasive *in vivo* detection of neuroaxonal pathology in multiple sclerosis. Future studies will extend the use of these techniques in cohorts with progressive disease and investigate, longitudinally, how the observed changes evolve over time.

Acknowledgements

Funding

Supplementary material

Supplementary material is available at *Brain* online.

References

Agosta F, Rovaris M, Pagani E, Sormani MP, Comi G, Filippi M. Magnetization transfer MRI metrics predict the accumulation of disability 8 years later in patients with multiple sclerosis. Brain 2006; 129: 2620–7.

Alonso-Ortiz E, Levesque IR, Pike GB. MRI-based myelin water imaging: a technical review. Magn Reson Med 2015; 73: 70–81.

Arshad M, Stanley JA, Raz N. Test–retest reliability and concurrent validity of *in vivo* myelin content indices: Myelin water fraction and calibrated T1w/T2w image ratio. Hum Brain Mapp 2017; 38: 1780–90.

Assaf Y, Blumenfeld-Katzir T, Yovel Y, Basser PJ. AxCaliber: a method for measuring axon diameter distribution from diffusion MRI. Magn Reson Med 2008; 59: 1347–54.

Assaf Y, Freidlin RZ, Rohde GK, Basser PJ. New modeling and experimental framework to characterize hindered and restricted water diffusion in brain white matter. Magn Reson Med 2004; 52: 965–78.

Bø L, Vedeler CA, Nyland HI, Trapp BD, Mørk SJ. Subpial demyelination in the cerebral cortex of multiple sclerosis patients. J Neuropathol Exp Neurol 2003; 62: 723–32.

Calabrese M, Atzori M, Bernardi V, Morra A, Romualdi C, Rinaldi L, et al. Cortical atrophy is relevant in multiple sclerosis at clinical onset. J Neurol 2007; 254: 1212–20.

Calabrese M, Castellaro M, Bertoldo A, De Luca A, Pizzini F, Ricciardi G, et al. Epilepsy in multiple sclerosis: the role of temporal lobe damage. Mult Scler J 2017; 23: 473–82.

Calabrese M, Filippi M, Gallo P. Cortical lesions in multiple sclerosis. Nat Rev Neurol 2010a; 6: 438–44.

Calabrese M, Reynolds R, Magliozzi R, Castellaro M, Morra A, Scalfari A, et al. Regional distribution and evolution of gray matter damage in different populations of multiple sclerosis patients. PLoS One 2015; 10: e0135428.

Calabrese M, Rinaldi F, Seppi D, Favaretto A, Squarcina L, Mattisi I, et al. Cortical diffusion-tensor imaging abnormalities in multiple sclerosis: a 3-year longitudinal study. Radiology 2011; 261: 891–8.

Calabrese M, Rocca MA, Atzori M, Mattisi I, Favaretto A, Perini P, et al. A 3-year magnetic resonance imaging study of cortical lesions in relapse-onset multiple sclerosis. Ann Neurol. 2010b; 67: 376–83.

Caverzasi E, Papinutto N, Castellano A, Zhu AH, Scifo P, Riva M, et al. Neurite orientation dispersion and density imaging color maps to characterize brain diffusion in neurologic disorders. J Neuroimaging 2016; 26: 494–8.

Chard D, Miller D. Grey matter pathology in clinically early multiple sclerosis: evidence from magnetic resonance imaging. J Neurol Sci 2009; 282: 5–11.

Chung AW, Seunarine KK, Clark CA. NODDI reproducibility and variability with magnetic field strength: a comparison between 1.5 T and 3 T. Hum Brain Mapp 2016; 37: 4550–65.

Cohen-Adad J, Benner T, Greve D, Kinkel RP, Radding A, Fischl B, et al. *In vivo* evidence of disseminated subpial T2* signal changes in multiple sclerosis at 7 T: a surface-based analysis. Neuroimage 2011; 57: 55–62.

Colgan N, Siow B, O'Callaghan JM, Harrison IF, Wells JA, Holmes HE, et al. Application of neurite orientation dispersion and density imaging (NODDI) to a tau pathology model of Alzheimer's disease. Neuroimage 2016; 125: 739–44.

Criste G, Trapp B, Dutta R. Axonal loss in multiple sclerosis: causes and mechanisms. Handb Clin Neurol 2014; 122: 101–13.

Daducci A, Canales-Rodríguez EJ, Zhang H, Dyrby TB, Alexander DC, Thiran J-P. Accelerated Microstructure Imaging via Convex Optimization (AMICO) from diffusion MRI data. Neuroimage 2015; 105: 32–44.

Fan Q, Witzel T, Nummenmaa A, Van Dijk KRA, Van Horn JD, Drews MK, et al. MGH-USC Human Connectome Project datasets with ultra-high b-value diffusion MRI. Neuroimage 2016; 124: 1108–14.

Fedorov A, Beichel R, Kalpathy-Cramer J, Finet J, Fillion-Robin J-C, Pujol S, et al. 3D Slicer as an image computing platform for the quantitative imaging network. Magn Reson Imaging 2012; 30: 1323–41.

Fick RHJ, Wassermann D, Caruyer E, Deriche R. MAPL: tissue microstructure estimation using Laplacian-regularized MAP-MRI and its application to HCP data. Neuroimage 2016; 134: 365–85.

Filippi M, Preziosa P, Pagani E, Copetti M, Mesaros S, Colombo B, et al. Microstructural magnetic resonance imaging of cortical lesions in multiple sclerosis. Mult Scler 2013; 19: 418–26.

Filippi M, Rocca MA, Barkhof F, Brück W, Chen JT, Comi G, et al. Association between pathological and MRI findings in multiple sclerosis. Lancet Neurol 2012; 11: 349–60.

Filippi M, Rocca MA, Ciccarelli O, Stefano ND, Evangelou N, Kappos L, et al. MRI criteria for the diagnosis of multiple sclerosis: MAGNIMS consensus guidelines. Lancet Neurol 2016; 15: 292–303.

Fischl B. FreeSurfer. Neuroimage 2012; 62: 774–81.

Friese MA, Schattling B, Fugger L. Mechanisms of neurodegeneration and axonal dysfunction in multiple sclerosis. Nat Rev Neurol 2014; 10: 225–38.

Fukunaga M, Li T-Q, van Gelderen P, de Zwart JA, Shmueli K, Yao B, et al. Layer-specific variation of iron content in cerebral cortex as a source of MRI contrast. Proc Natl Acad Sci USA 2010; 107: 3834–9.

Ganzetti M, Wenderoth N, Mantini D. Whole brain myelin mapping using T1- and T2-weighted MR imaging data. Front Hum Neurosci 2014; 8: 671.

Ganzetti M, Wenderoth N, Mantini D. Mapping pathological changes in brain structure by combining T1- and T2-weighted MR imaging data. Neuroradiology 2015; 57: 917–28.

Giorgio A, Stromillo ML, Rossi F, Battaglini M, Hakiki B, Portaccio E, et al. Cortical lesions in radiologically isolated syndrome. Neurology 2011; 77: 1896–9.

Glasser MF, Coalson TS, Robinson EC, Hacker CD, Harwell J, Yacoub E, et al. A multi-modal parcellation of human cerebral cortex. Nature 2016; 536: 171–8.

Glasser MF, Goyal MS, Preuss TM, Raichle ME, Van Essen DC. Trends and properties of human cerebral cortex: correlations with cortical myelin content. Neuroimage 2014; 93: 165–75.

Glasser MF, Van Essen DC. Mapping human cortical areas *in vivo* based on myelin content as revealed by T1- and T2-weighted MRI. J Neurosci 2011; 31: 11597–616.

Govindarajan ST, Cohen-Adad J, Sormani MP, Fan AP, Louapre C, Mainero C. Reproducibility of T2* mapping in the human cerebral cortex *in vivo* at 7 Tesla MRI. J Magn Reson Imaging 2015; 42: 290–6.

Greve DN, Fischl B. Accurate and robust brain image alignment using boundary-based registration. Neuroimage 2009; 48: 63–72.

Guo AC, MacFall JR, Provenzale JM. Multiple sclerosis: diffusion tensor MR imaging for evaluation of normal-appearing white matter. Radiology 2002; 222: 729–36.

Guttmann CR, Rousset M, Roch JA, Hannoun S, Durand-Dubief F, Belaroussi B, et al. Multiple sclerosis lesion formation and early evolution revisited: a weekly high-resolution magnetic resonance imaging study. Mult Scler 2016; 22: 761–9.

Haider L, Zrzavy T, Hametner S, Höftberger R, Bagnato F, Grabner G, et al. The topograpy of demyelination and neurodegeneration in the multiple sclerosis brain. Brain 2016; 139: 807–15.

Harrison DM, Roy S, Oh J, Izbudak I, Pham D, Courtney S, et al. Association of cortical lesion burden on 7-T magnetic resonance imaging with cognition and disability in multiple sclerosis. JAMA Neurol 2015; 72: 1004–12.

Henderson G, Tomlinson BE, Gibson PH. Cell counts in human cerebral cortex in normal adults throughout life using an image analysing computer. J Neurol Sci 1980; 46: 113–36.

Jelescu IO, Zurek M, Winters KV, Veraart J, Rajaratnam A, Kim NS, et al. *In vivo* quantification of demyelination and recovery using compartment-specific diffusion MRI metrics validated by electron microscopy. Neuroimage 2016; 132: 104–14.

Jonkman LE, Klaver R, Fleysher L, Inglese M, Geurts JJ. The substrate of increased cortical FA in MS: a 7T post-mortem MRI and histopathology study. Mult Scler 2016; 22: 1804–11.

Kaden E, Kelm ND, Carson RP, Does MD, Alexander DC. Multi-compartment microscopic diffusion imaging. Neuroimage 2016; 139: 346–59.

Kamagata K, Hatano T, Okuzumi A, Motoi Y, Abe O, Shimoji K, et al. Neurite orientation dispersion and density imaging in the substantia nigra in idiopathic Parkinson disease. Eur Radiol 2015; 26: 2567–77.

Keil B, Blau JN, Biber S, Hoecht P, Tountcheva V, Setsompop K, et al. A 64-channel 3T array coil for accelerated brain MRI. Magn Reson Med 2013; 70: 248–58.

Kilsdonk ID, Jonkman LE, Klaver R, van Veluw SJ, Zwanenburg JJM, Kuijer JPA, et al. Increased cortical grey matter lesion detection in multiple sclerosis with 7 T MRI: a post-mortem verification study. Brain 2016; 139: 1472–81.

Kuhlmann T, Lingfeld G, Bitsch A, Schuchardt J, Brück W. Acute axonal damage in multiple sclerosis is most extensive in early disease stages and decreases over time. Brain 2002; 125: 2202–12.

Kurtzke JF. Rating neurologic impairment in multiple sclerosis: an expanded disability status scale (EDSS). Neurology 1983; 33: 1444–52.

Lassmann H. Pathology and disease mechanisms in different stages of multiple sclerosis. J Neurol Sci 2013; 333: 1–4.

Louapre C, Govindarajan ST, Giannì C, Langkammer C, Sloane JA, Kinkel RP, et al. Beyond focal cortical lesions in MS: an *in vivo* quantitative and spatial imaging study at 7T. Neurology 2015; 85: 1702–9.

Louapre C, Perlbarg V, García-Lorenzo D, Urbanski M, Benali H, Assouad R, et al. Brain networks disconnection in early multiple sclerosis cognitive deficits: an anatomofunctional study. Hum Brain Mapp 2014; 35: 4706–17.

Lublin FD, Reingold SC, Cohen JA, Cutter GR, Sørensen PS, Thompson AJ, et al. Defining the clinical course of multiple sclerosis: the 2013 revisions. Neurology 2014; 83: 278–86.

Lucchinetti CF, Popescu BFG, Bunyan RF, Moll NM, Roemer SF, Lassmann H, et al. Inflammatory cortical demyelination in early multiple sclerosis. N Engl J Med 2011; 365: 2188–97.

Mainero C, Benner T, Radding A, van der Kouwe A, Jensen R, Rosen BR, et al. *In vivo* imaging of cortical pathology in multiple sclerosis using ultra-high field MRI. Neurology 2009; 73: 941–8.

Mainero C, Louapre C, Govindarajan ST, Giannì C, Nielsen AS, Cohen-Adad J, et al. A gradient in cortical pathology in multiple sclerosis by *in vivo* quantitative 7 T imaging. Brain 2015; 138: 932–45.

Mangeat G, Govindarajan ST, Mainero C, Cohen-Adad J. Multivariate combination of magnetization transfer, T2* and B0 orientation to study the myelo-architecture of the *in vivo* human cortex. Neuroimage 2015; 119: 89–102.

McNab JA, Edlow BL, Witzel T, Huang SY, Bhat H, Heberlein K, et al. The Human Connectome Project and beyond: initial applications of 300 mT/m gradients. Neuroimage 2013; 80: 234–45.

Morris LS, Kundu P, Dowell N, Mechelmans DJ, Favre P, Irvine MA, et al. Fronto-striatal organization: defining functional and microstructural substrates of behavioural flexibility. Cortex 2016; 74: 118–33.

Nakamura K, Chen J, Fox R, Ontaneda D, Trapp BD. Imaging cortical demyelination using T1/T2-weighted ratio. Mult Scler J 2016; 22: 400–5.

Nielsen AS, Kinkel RP, Tinelli E, Benner T, Cohen-Adad J, Mainero C. Focal cortical lesion detection in multiple sclerosis: 3 Tesla DIR versus 7 Tesla FLASH-T2. J Magn Reson Imaging 2012; 35: 537–42.

Nygaard GO, Walhovd KB, Sowa P, Chepkoech J-L, Bjørnerud A, Due-Tønnessen P, et al. Cortical thickness and surface area relate to specific symptoms in early relapsing-remitting multiple sclerosis. Mult Scler 2015; 21: 402–14.

MAGNIMS study Group. Evidence-based guidelines: MAGNIMS consensus guidelines on the use of MRI in multiple sclerosis—establishing disease prognosis and monitoring patients. Nat Rev Neurol 2015; 11: 597–606.

Pantano P, Iannetti GD, Caramia F, Mainero C, Di Legge S, Bozzao L, et al. Cortical motor reorganization after a single clinical attack of multiple sclerosis. Brain 2002; 125: 1607–15.

Pareto D, Sastre-Garriga J, Auger C, Vives-Gilabert Y, Delgado J, Tintoré M, et al. Juxtacortical lesions and cortical thinning in multiple sclerosis. AJNR Am J Neuroradiol 2015; 36: 2270–6.

Peterson JW, Bö L, Mörk S, Chang A, Trapp BD. Transected neurites, apoptotic neurons, and reduced inflammation in cortical multiple sclerosis lesions. Ann Neurol 2001; 50: 389–400.

Pitt D, Boster A, Pei W, Wohleb E, Jasne A, Zachariah CR, et al. Imaging cortical lesions in multiple sclerosis with ultra-high-field magnetic resonance imaging. Arch Neurol 2010; 67: 812–18.

Polman CH, Reingold SC, Banwell B, Clanet M, Cohen JA, Filippi M, et al. Diagnostic criteria for multiple sclerosis: 2010 revisions to the McDonald criteria. Ann Neurol 2011; 69: 292–302.

Poonawalla AH, Hasan KM, Gupta RK, Ahn CW, Nelson F, Wolinsky JS, et al. Diffusion-tensor MR imaging of cortical lesions in multiple sclerosis: initial findings. Radiology 2008; 246: 880–6.

Reisert M, Kellner E, Dhital B, Hennig J, Kiselev VG. Disentangling micro from mesostructure by diffusion MRI: a Bayesian approach. Neuroimage 2017; 147: 964–75.

Rocca MA, Falini A, Colombo B, Scotti G, Comi G, Filippi M. Adaptive functional changes in the cerebral cortex of patients with nondisabling multiple sclerosis correlate with the extent of brain structural damage. Ann Neurol 2002; 51: 330–9.

Rovira À, Wattjes MP, Tintoré M, Tur C, Yousry TA, Sormani MP, et al. Evidence-based guidelines: MAGNIMS consensus guidelines on the use of MRI in multiple sclerosis-clinical implementation in the diagnostic process. Nat Rev Neurol 2015; 11: 471–82.

Schmierer K, Wheeler-Kingshott CAM, Boulby PA, Scaravilli F, Altmann DR, Barker GJ, et al. Diffusion tensor imaging of post mortem multiple sclerosis brain. Neuroimage 2007; 35: 467–77.

Setsompop K, Kimmlingen R, Eberlein E, Witzel T, Cohen-Adad J, McNab JA, et al. Pushing the limits of *in vivo* diffusion MRI for the Human Connectome Project. Neuroimage 2013; 80: 220–33.

Simon J. Very early MS—insights from MRI. Mult Scler 2012; 18: 1372–6.

Sotiropoulos SN, Behrens TEJ, Jbabdi S. Ball and rackets: inferring fiber fanning from diffusion-weighted MRI. Neuroimage 2012; 60: 1412–25.

Steenwijk MD, Daams M, Pouwels PJW, Balk LJ, Tewarie PK, Killestein J, et al. What explains gray matter atrophy in long-standing multiple sclerosis? Radiology 2014; 272: 832–42.

Stikov N, Campbell JSW, Stroh T, Lavelée M, Frey S, Novek J, et al. *In vivo* histology of the myelin g-ratio with magnetic resonance imaging. Neuroimage 2015; 118: 397–405.

Traboulsee A, Simon JH, Stone L, Fisher E, Jones DE, Malhotra A, et al. Revised recommendations of the consortium of MS Centers Task Force for a standardized MRI protocol and clinical guidelines for the diagnosis and follow-up of multiple sclerosis. AJNR Am J Neuroradiol 2016; 37: 394–401.

Trapp BD, Nave K-A. Multiple sclerosis: an immune or neurodegenerative disorder? Annu Rev Neurosci 2008; 31: 247–69.

Trapp BD, Peterson J, Ransohoff RM, Rudick R, Mörk S, Bö L. Axonal transection in the lesions of multiple sclerosis. N Engl J Med 1998; 338: 278–85.

van der Kouwe AJW, Benner T, Salat DH, Fischl B. Brain morphometry with multiecho MPRAGE. Neuroimage 2008; 40: 559–69.

Vrenken H, Pouwels PJW, Ropele S, Knol DL, Geurts JJG, Polman CH, et al. Magnetization transfer ratio measurement in multiple sclerosis normal-appearing brain tissue: limited differences with controls but relationships with clinical and MR measures of disease. Mult Scler 2007; 13: 708–16.

Yaldizli Ö, Pardini M, Sethi V, Muhlert N, Liu Z, Tozer DJ, et al. Characteristics of lesional and extra-lesional cortical grey matter in relapsing–remitting and secondary progressive multiple sclerosis: a magnetisation transfer and diffusion tensor imaging study. Mult Scler 2016; 22: 150–9.

Zhang H, Schneider T, Wheeler-Kingshott CA, Alexander DC. NODDI: practical *in vivo* neurite orientation dispersion and density imaging of the human brain. Neuroimage 2012; 61: 1000–16.